









The application of numerical simulations to analyze the forward extrusion process along with the verification of results and tuning of the numerical model

Marek Hawryluk^{1,2*} , Łukasz Dudkiewicz^{1,3} , Jan Marzec¹ , Roger Tkocz⁴ ,
Jacek Borowski⁵ , Grzegorz Ficak⁶ , Bartosz Józwiak⁷ , Jacek Ziemba^{1,2} 

¹ Wrocław University of Science and Technology, Department of Metal Forming, Welding and Metrology, Wrocław, Poland.

² Center for Materials Science and Metal Forming, Wrocław, Poland.

³ Schraner Polska sp. z o.o., Łęczyca, Poland.

⁴ MAHLE Behr Poland, Ostrów Wielkopolski, Poland.

⁵ The Łukasiewicz Research Network – Poznań Institute of Technology, Poznań, Poland.

⁶ GK FORGE sp. z o.o., Goleszów, Poland.

⁷ GKN Driveline Polska sp. z o.o., Oleśnica, Poland.

Abstract

The paper presents the application of numerical simulations based on the Finite Element Method (FEM) for analyzing and optimizing the extrusion processes of aluminum and lead. These processes are efficient methods for manufacturing critical machine parts and metal components, ensuring excellent mechanical properties. A detailed analysis was conducted on the numerical modeling of the impact of die taper angles on strain distribution and forming forces during co-extrusion. The study found that a 45-degree angle provides optimal deformation conditions, minimizing extrusion forces and reducing the formation of dead zones compared to a 90-degree angle. Numerical simulations, supplemented by technological trials under semi-industrial conditions and image analysis involving the deformation of the coordinate grid, provided key insights into a material flow, strain distribution, and force parameters. The results emphasize the importance of validating numerical models with semi-industrial experiments to ensure accuracy and reliability, as assuming constant tribological conditions may not reflect actual process conditions, including the formation of dead zones for angles greater than 45°. It was only through a thorough analysis of the actual process and the introduction of variable friction coefficients for individual tools that a dead zone was achieved in the modelling. The findings from this research can serve as the foundation for further optimization and adaptation of technological processes, aiming to further enhance extrusion processes through the use of numerical simulations.

Keywords: forward extrusion process, FE modelling, die draft angle, dead zone, aluminum and lead

1. Introduction

In recent years, there has been a rapid development of energy-efficient technologies for manufacturing high-quality products based on plastic forming processes, which

include forging and the extrusion of components dedicated to critical machine parts (Leśniak et al., 2024). Extrusion is one of the most economical methods among plastic forming processes and serves as a primary technique for manufacturing tubes, rods, profiles, and machine parts

* Corresponding author: marek.hawryluk@pwr.edu.pl

ORCID ID's: 0000-0002-9338-4327 (M. Hawryluk), 0009-0000-0191-7687 (Ł. Dudkiewicz), 0000-0003-4127-3315 (J. Marzec), 0009-0006-7195-8998 (R. Tkocz), 0000-0002-5983-3096 (J. Borowski), 0009-0005-9271-1284 (G. Ficak), 0009-0007-8982-4696 (B. Józwiak), 0000-0002-3505-7555 (J. Ziemba)

© 2025 Authors. This is an open access publication, which can be used, distributed and reproduced in any medium according to the Creative Commons CC BY 4.0 License requiring that the original work has been properly cited.

from steel and non-ferrous metals. Extruded products are characterized by excellent mechanical properties, high dimensional accuracy, and clean, smooth surfaces. Industrial extrusion processes are crucial for producing rods and tubes, which have broad applications across various industries, ranging from automotive to construction (Khalid et al., 2023). Aluminum, valued for its lightness and corrosion resistance, is particularly prized in the production of extruded components for the aerospace and automotive industries. It is also used in creating profiles with complex shapes and excellent mechanical properties for various industrial sectors (Zhang et al., 2012). Lead, on the other hand, due to its density and ease of forming, is often employed in the production of pipes and rods used in applications such as radiation shielding and battery components. The extrusion processes for lead require precise control of parameters to ensure the appropriate quality and strength of the final product (Soydan et al., 2024).

Currently, numerical modeling based on mathematical apparatus and new computational techniques (mainly using FEM) that have developed rapidly recently, as well as methods based on experimentation are used to design and analyze real plastic forming processes, including extrusion processes (Madej et al., 2015). The most important of these are physical modelling and simulation, as well as the physical modelling of forging and extrusion processes (Vazques et al., 2000). These methods can serve as an independent tool in the design of plastic processing processes, taking into account both the shape and properties of the final product. They can also collaborate with mathematical modelling, providing essential information about the physical properties of the deformed material, boundary conditions, and structural changes, and can act as a verification tool (Hawryluk et al., 2023). The most crucial stage of design is the final verification of the developed plastic forming process on the actual material. The success of the designed plastic processing methods largely depends on the skills and experience of process engineers and technologists. Therefore, in the case of designing and optimizing existing processes, a comprehensive analysis of industrial aluminum (Brough & Jouhara, 2020) and lead (Çalım et al., 2023) extrusion processes through the use of numerical modelling is essential because it is crucial for the optimization of modern production technologies. Numerical simulations play a crucial role in the analysis and optimization of extrusion parameters, such as temperature, piston speed, and die geometry (Chan et al., 2008). Numerical models also enable the simulation of metal flow, which is crucial

for ensuring uniform stress distribution and minimizing material losses (Williams et al., 2002). Numerical modelling can also help predict the impact of different process conditions on the final properties of products, which is invaluable in designing new products and optimizing existing processes (Campana et al., 2010). Hence, the use of computer simulations using FEM enables the optimization of both the entire plastic processing process and specific phenomena, such as the shape of the dies used in extrusion processes (Ji et al., 2023). It is also often assumed that a significant part of the machining processes carried out in engineering practice can be analyzed without making major mistakes after assuming simplified states of strain or stress, such as: plane strain state, axisymmetric strain state, and plane stress state. The adoption of such simplifications allows, on the one hand, to shorten the calculation time, but on the other hand, it may introduce additional errors for inexperienced researchers, which may be difficult to diagnose and interpret the obtained results (Chenot et al., 2010).

It should be emphasized that the use of numerical modeling in the processes of aluminum and lead extrusion contributes to increasing the innovativeness and competitiveness of enterprises (Donati et al., 2022). This not only reduces costs, but also improves the quality and durability of products, which is crucial in the context of sustainable development and energy efficiency (Liu & Müller, 2012). In the future, further development of numerical simulation techniques may lead to even greater precision and efficiency of extrusion processes, which is extremely important in the dynamically changing industrial environment (He et al., 2012). The introduction of new technologies, such as machine learning and artificial intelligence, can further improve modeling and optimization processes (Negozio et al., 2024). By combining advanced industrial analysis with modern modelling techniques, it is possible to achieve a higher level of control over production processes (Kochański et al., 2024). This, in turn, leads to increased product quality, reduced waste and increased overall production efficiency through automation and robotics (Hawryluk & Rychlik, 2022). The introduction of innovative technological solutions in extrusion processes lays the foundation for the future development of the metallurgical industry and its adaptation to global environmental challenges (Oberhausen et al., 2022). As extrusion and numerical modelling technology continues to advance, it is possible to create more advanced and complex products that meet the growing demands of the market (Hu et al., 2012). Therefore, the use of the entire spectrum of re-

search methods based on CAD/CAM/CAE/RP (Yang et al., 2002) and non-destructive tests (3D scanning, thermal imaging measurements, etc.) and destructive tests (material and microstructural tests) as well as various computational techniques based on FEM/FVM is fully justified (Hawryluk et al., 2023). This comprehensive approach allows for mutual verification of research, which reduces the costs of industrial verification, and on the other hand, allows for easier and faster solution of many research problems, e.g. related to the correct implementation and optimization of extrusion processes.

This work aims to apply the results of numerical modelling to analyze the influence of the die taper angle on the distribution of strains and forming forces in the process of co-extrusion of lead, as well as to tune the parameters during numerical modelling of aluminum extrusion and the formation of the dead zone based on technological tests in semi-industrial conditions.

2. Research subject and methodology

The analysis was performed on the co-extrusion process for two materials: lead and aluminum, for which a thermomechanical numerical model of extrusion in a plane strain state was built. Co-extrusion in a plane strain state is shown in Figure 1a.

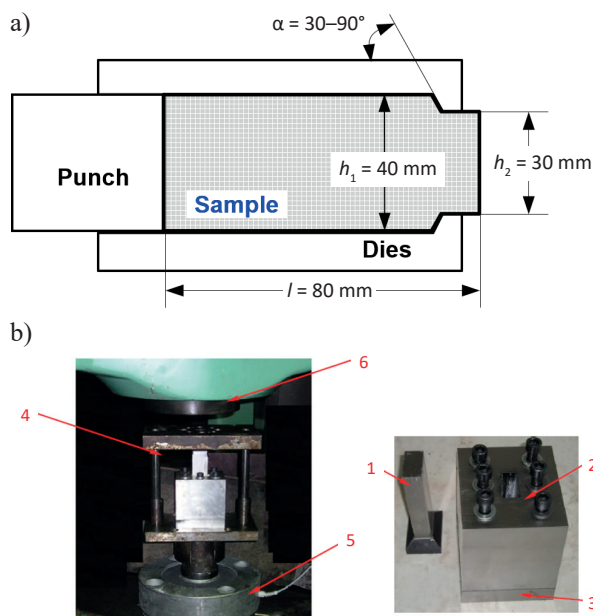


Fig. 1. The view of: a) forward extrusion in plane strain state: l – initial sample length, h_1 – sample width, h_2 – die width, α – die angle; b) photo of the laboratory stand to extrusion process in semi-industrial conditions: 1 – stamp, 2 – chamber, 3 – mold (die), 4 – device casing, 5 – load detector, 6 – hydraulic press

The research was divided into two main stages. The first stage involved the forward extrusion process of lead and the analysis of the effect of the convergence angle. During the technological trials for this process, the formation of a dead zone in the die was observed, especially at large angles (above 45°), which was not evident in numerical modelling. Therefore, a second stage of research was conducted, focusing on fine-tuning the numerical model of the co-extrusion process for aluminum. This was based on the experience of co-extruding aluminum using steel tools under semi-industrial conditions. Figure 1b illustrates the experimental setup for co-extrusion of both materials under semi-industrial conditions (tools mounted on a press with a force of 2,000 kN, equipped with a force sensor with a range of 1,000 kN). It was decided to choose these materials because, on the one hand, they represent two groups of plastic working processes: Aluminum formed at an ambient temperature is classified as cold plastic working (material strengthening), while extrusion of Pb at an ambient temperature is hot plastic working. In turn, Al, due to its high immediate strength and corrosion resistance, is particularly valued in the production of components for the aerospace and automotive industries. On the other hand, Pb, thanks to its density and ease of forming, is often used as a model material that simulates the hot deformation of steel well, and as a target material, it is intended for applications in radiation shields and battery components.

3. Development of a numerical model

The thermo-mechanical mathematical model of the extrusion process was developed using the Marc Mentat 2015 software. MSC software allows for the simulation of material forming processes, including extrusion and analysis of structural changes during cooling. The program also enables microstructure analysis. For discretizing the deformable material, 1,200 quadrilateral Solid 11 (Quad 4) elements were used. The model employed automatic remeshing, adjusting the number and distribution of element density due to deformation and tool penetration. In the numerical model of the reinforced aluminum extrusion process, all tools – die, punch, and container – were assumed to be rigid. The stress-strain curves for lead and aluminum were inputted numerically for different strain rates, determined in a uniaxial compression test (Fig. 2). The chemical composition of both materials is shown in Table 1.

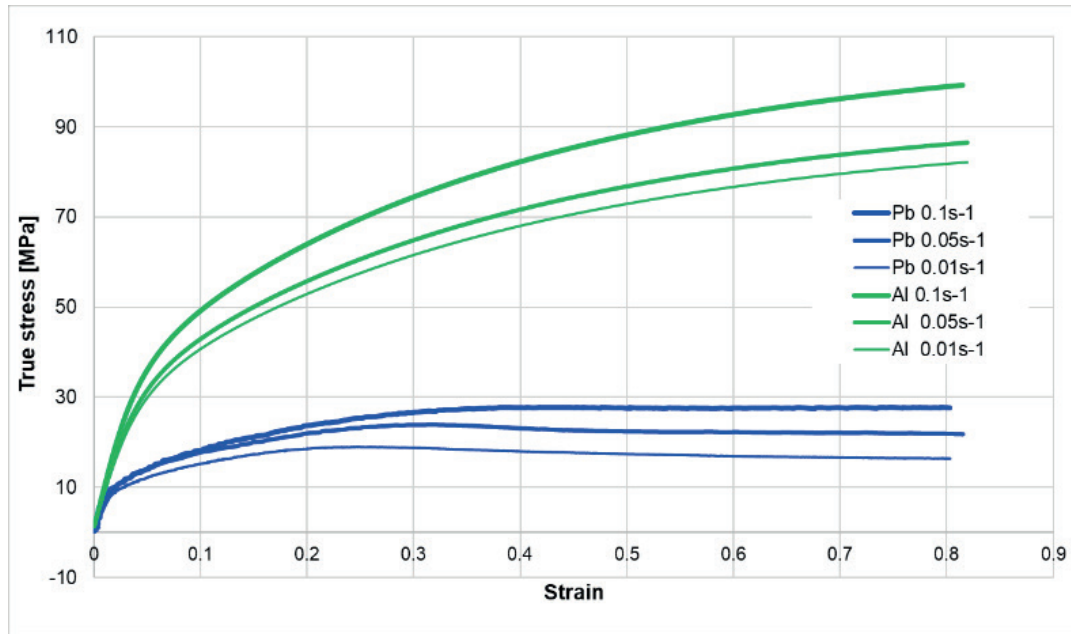


Fig. 2. The overview of flow true stress-strain curves for selected metallic materials, representing different variants of metal forming processes: lead (hot forming), aluminum (cold forming)

Table 1. Chemical composition of used materials [%]

Al	Fe	Si	Cu	Mn	Mg	Zn	Ti
≥99.5	≤0.40	≤0.25	≤0.05	≤0.05	≤0.05	≤0.07	≤0.03
Pb	Cu	Bi	As	Sb	Sn	Fe	Zn
≥99.97	≤0.01	≤0.01	≤0.005	≤0.005	≤0.005	≤0.005	≤0.005

Boundary conditions were set to closely resemble those of the actual process. The Coulomb friction model was applied, with a constant friction coefficient of 0.05 for all tools, determined from a ring test. The following heat transfer coefficients were used: for Pb – specific heat of 0.13 kJ/(kg·K) and thermal conductivity of 36 W/(m·K); for Al – specific heat of 0.86 kJ/(kg·K) and thermal conductivity of 240 W/(m·K). For steel tools, the specific heat was assumed to be 0.46 kJ/(kg·K) and thermal conductivity 305 W/(m·K). These are literature data that can also be found online (The Engineering ToolBox, 2003).

4. Research results and discussion

4.1. Forward extrusion of Pb

The following sample geometry was assumed in numerical modeling: initial length ($l_o = 80$ mm), half-sample width ($1/2s_o = 20$ mm), and thickness (in plane deformation state, $g_o = 20$ mm). The punch speed in both the numerical modelling and experimental trials was set at 1.2 mm/s.

The extrusion ratio was determined using the following formula:

$$\text{Extrusion ratio} = \frac{A_o}{A_f} = \frac{40 \times 20}{30 \times 20} = \frac{800}{600} = 1.33 \quad (1)$$

where:

A_o – cross-sectional area of the billet (before the process),

A_f – cross-sectional area of the extrudate (after extrusion).

In order to shorten the calculation time, half of the model was analyzed using the process symmetry. Figure 3a shows extrusion diagrams for the tool variant with a die convergence angle of 30°. In turn, Figure 3b shows an example photo of a deformed sample with flow lines turned on (square mesh with a side of 5 mm), which will allow for a comparison of the material flow from numerical modeling with the experiment.

Figure 4 shows the von Mises stress distributions (at the beginning and at the end of extrusion), while Figure 4b presents the unit pressures of the extruded material on the tool walls (die and recipient) for the co-extrusion process of lead with a draft angle of 30° in order to provide more comprehensive information on the strength parameters.

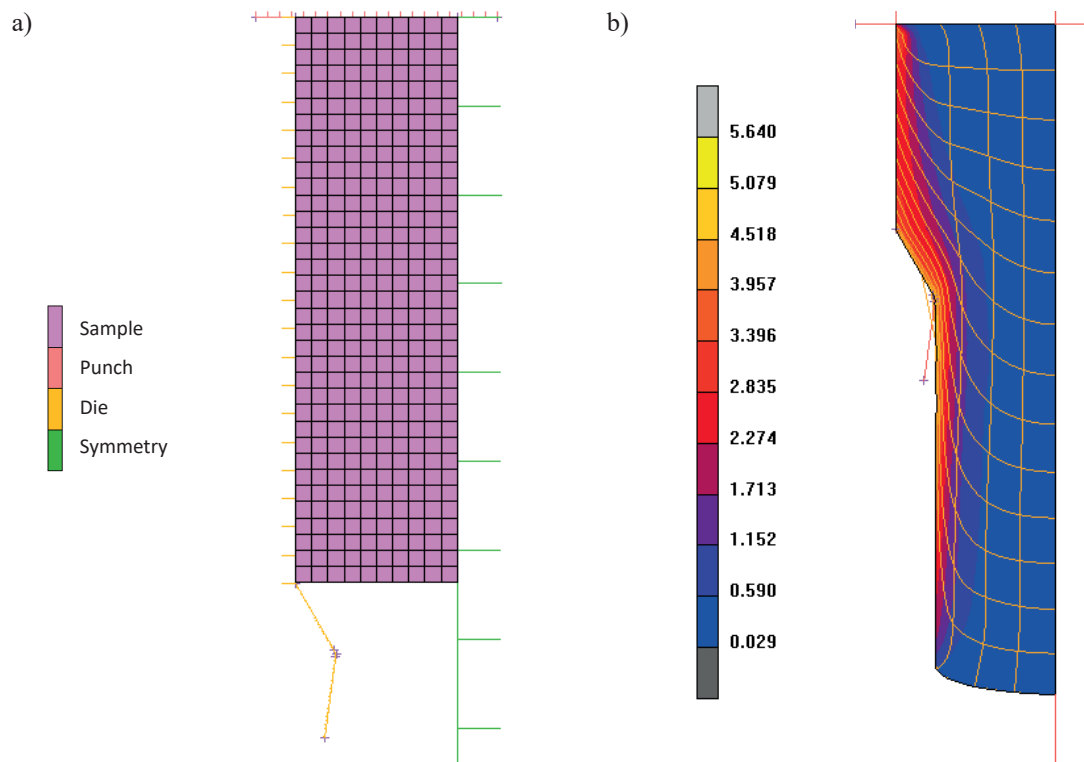


Fig. 3. Results of numerical simulations: a) scheme of co-extrusion of lead in plane strain state; b) deformed sample with material flow lines

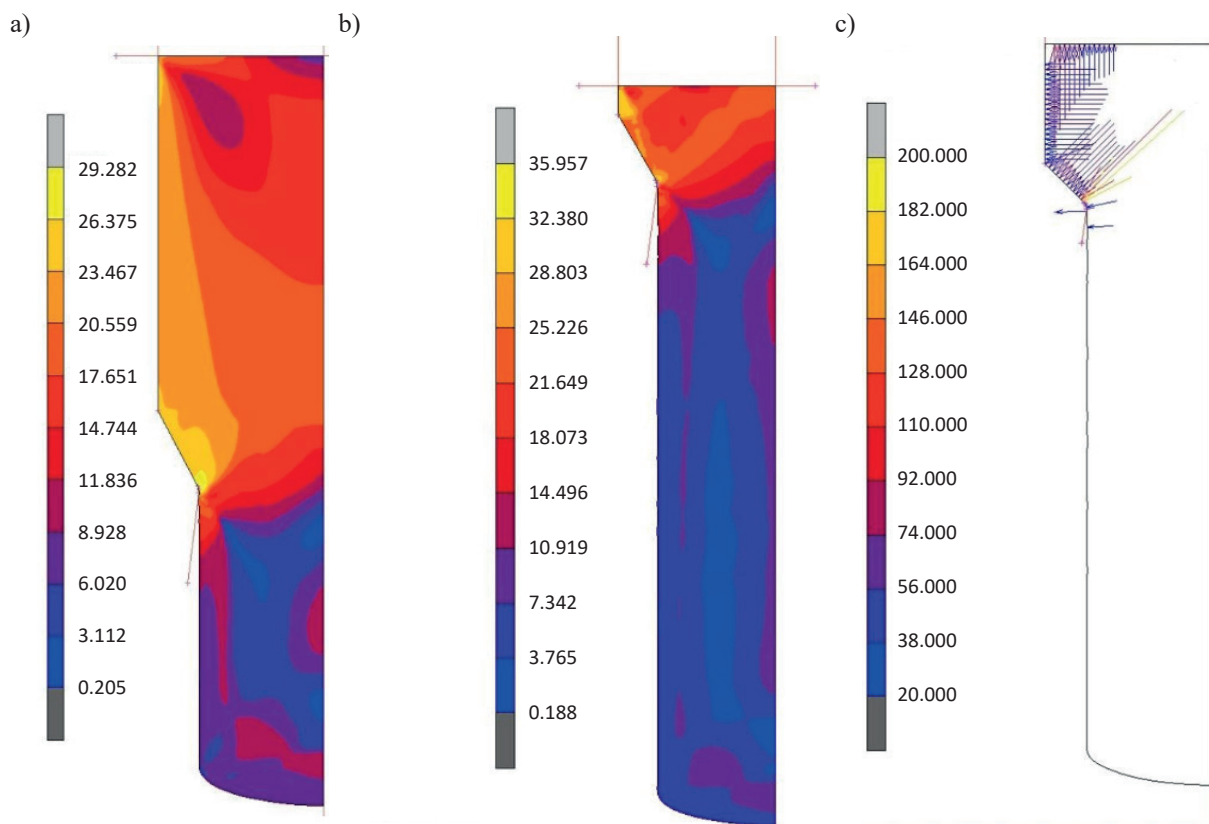


Fig. 4. FEM results: a) distributions of the equivalent von Mises stress in the initial phase of the process; b) distributions of the equivalent von Mises stress in the final phase of extrusion for a die taper angle of 30°; c) distributions of unit pressures in the final phase of the process

The presented results of numerical simulations allow for the selection and development of an appropriate tool design for other processes carried out in laboratory conditions. It can be seen that both the distributions of equivalent stresses and unit pressures are not very high for lead extrusion, which is caused by the low value of the yield strength of this material and the relatively small reduction in the extrusion process. On this basis, new extrusion dies can be made for other draft angles, assuming the same recipient. Based on the initial models, their correctness was verified through an experiment conducted under laboratory conditions. Then, further numerical models were built for different draft angles of dies (30° , 45° and 90°). Figure 5 shows the distributions of equivalent plastic strain and the material flow method for the analyzed draft angles of the die.

Analyzing the strain distributions, it can be seen that the greatest plastic strains occur for the right angle of the die convergence. This may be due to the difficulty in material flow near the dead zone located in the corner of the die. The shearing of the material could have forced the occurrence of large plastic strains in the shear zone. In turn, analyzing the flow lines, it can be seen that at the beginning of the sample, the lines are the least deformed in the case of an angle of 90° and vice versa for smaller angles. On the other hand,

in the subsequent areas (closer to the die eye), it can be observed that the least deformed flow lines occur for smaller angles of convergence (30° and 45°). The greatest deformation—bends of the flow lines can be observed for the right angle of the die convergence. Such a way of material flow indicates an uneven distribution of strain—material flow, and it is unfavorable because the extruded material is characterized by a non-uniform degree of deformation, which translates into the material structure and its various properties along the length. Figure 6 shows the extrusion forces as a function of the punch path for different taper angles.

In the case of extrusion forces, it can be observed that the average values of forces for the same conditions in FEM are the lowest for the 45° -degree angle, while the highest average forces can be observed for the right angle, where a dead zone is probably created in the corner. Slightly higher forces are also observed for the 30° -degree angle of convergence, which is caused by the longer die surface, which translates into greater friction and, consequently, a slightly higher force. In the case of numerical modelling, no clear dead zone was observed, although, at angles higher than 60° , such a zone should appear in the case of the laboratory experiment, where a large dead zone should be expected for the right angle.

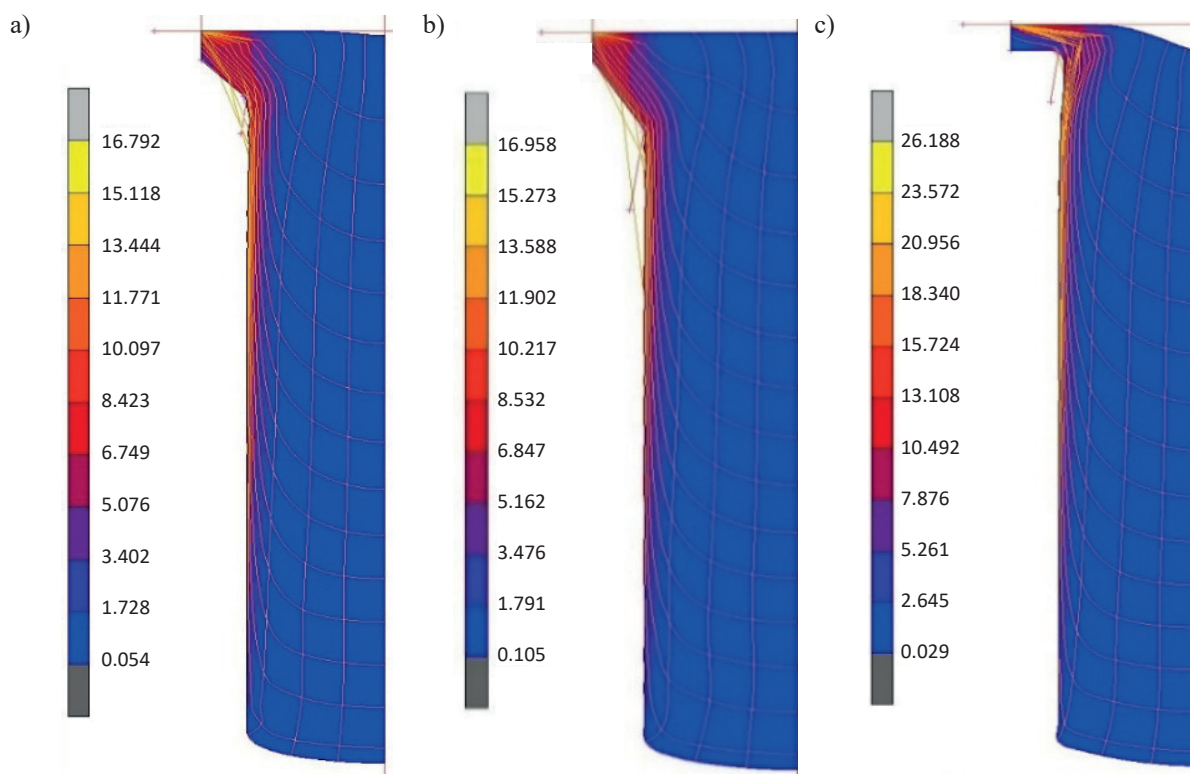


Fig. 5. Comparison of the distributions of equivalent plastic strain in the final phase of extrusion together with the flow lines for the analyzed die taper angles

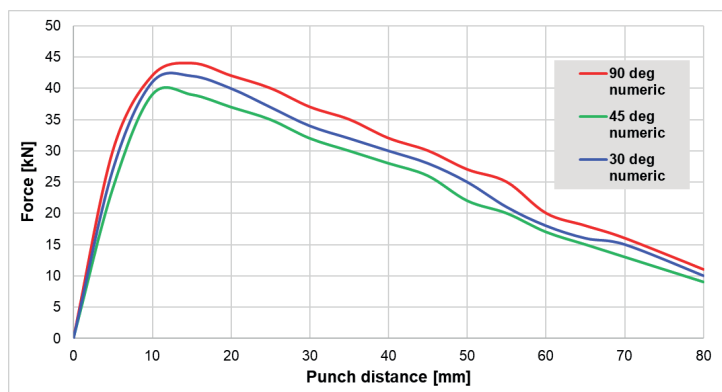


Fig. 6. Extrusion forces as a function of punch path for different die convergence angles obtained from FEM

4.2. Verification of the results of the forward extrusion process in semi-industrial conditions

In order to confirm the results of the numerical modelling, the process of co-rotating extrusion in a plane strain state was carried out. The starting material was in the form of samples consisting of two cuboids with dimensions of 10 mm × 40 mm × 70 mm made of lead. A coordination grid with a side of 10 mm was applied on the contact surface of both cuboids, which was used to determine the strain distribution. The extrusion process was carried out for the same three draft angles as in FEM (30°, 45°, 90°) at a temperature of 22°C and at a punch speed of 0.2 mm/s, which corresponded to an average strain rate of 0.01 s⁻¹. First, the numerical modelling was verified for the extrusion process for tools with a draft angle of 30°. A coordination grid with

a side of 5 mm was applied on the contact surface of both cuboids (Fig. 7a), which was used to determine the strain distribution using the ASUME program (Fig. 7b).

As can be seen, the obtained deformations are uniform, and the material's way is correct, resembling a calm laminar flow, which results from good lubrication (tribological) conditions. The largest deformations are located on the edges of the sample, where the material flowed most intensively, which is also confirmed by the bends of the grid lines. The smallest deformations are located in the central part as well as in the initial area of the sample – the beginning of the extrusion process – the inner radius of the mesh (R_A) is close to ∞ , and there is a relatively small bending of the lines in the outer part of the sample (R_o). Figure 8 shows the deformed coordination grids for the tested real materials. Based on the macroscopic analysis, differences in the flow method of individual materials were observed.

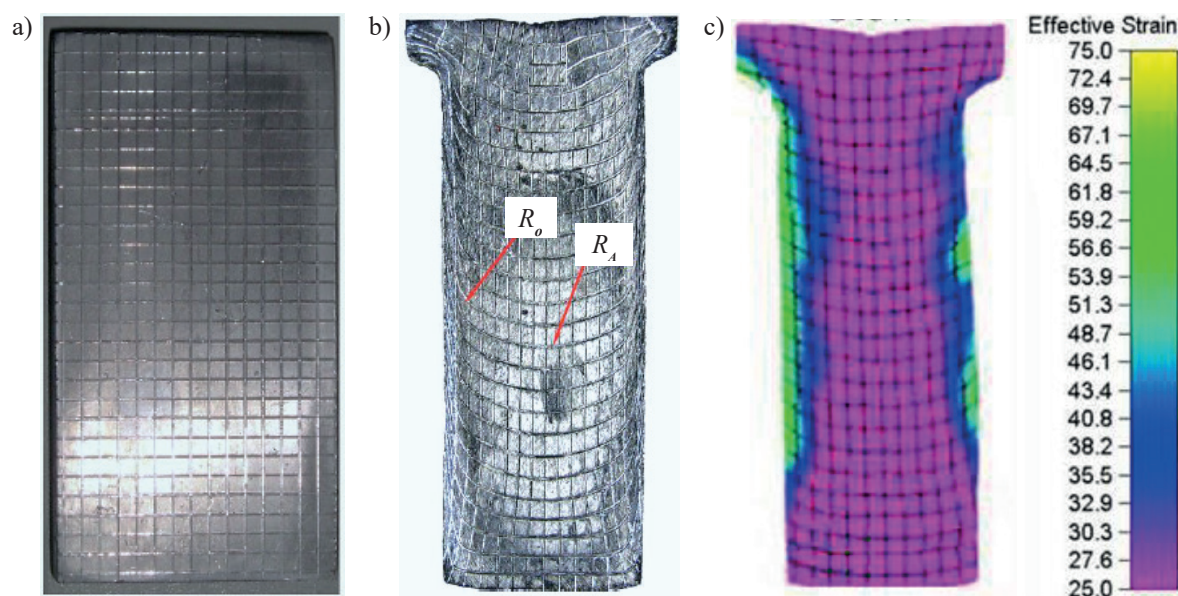


Fig. 7. The view of: a) sample with a coordination grid for co-extrusion in a plane strain state; b) extruded Pb sample; c) determined strain distributions on the surface using the ASUME program

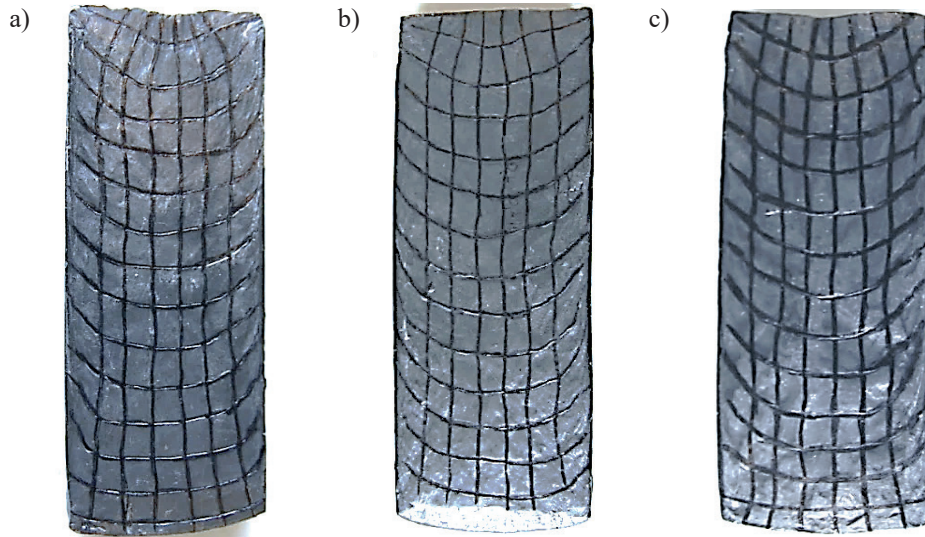


Fig. 8. Comparison of deformed meshes for samples deformed for different die draft angles; deformed sample for an angle of: a) 30°; b) 45°; c) 90°

For a 30-degree taper angle (Fig. 8a), the material deformation distribution is very uniform in the sample cross-section. This is evidenced by the constant bending of the coordination grid lines perpendicular to the extrusion direction. In the case of a 45-degree taper angle (Fig. 8b), the deformation is located mainly in the areas close to the die. The radius of curvature of the coordination grid lines perpendicular to the extrusion direction in the central part of the sample. However, in the case of the radii of curvature of the lines at the outer walls of the sample, the situation is reversed. The lead sample with

a right angle of the die taper (Fig. 8c) is characterized by the most uneven flow pattern, as evidenced by small bends of the coordination grid lines in the area of the central part of the sample. The next stage of the study involved comparing the flow patterns of deformed samples from numerical modelling and laboratory experiments for different die taper angles, in order to verify the FEM results under industrial conditions. Figure 9 shows a comparison of the flow behavior of deformed samples from numerical modeling and laboratory experiments for different die convergence angles.

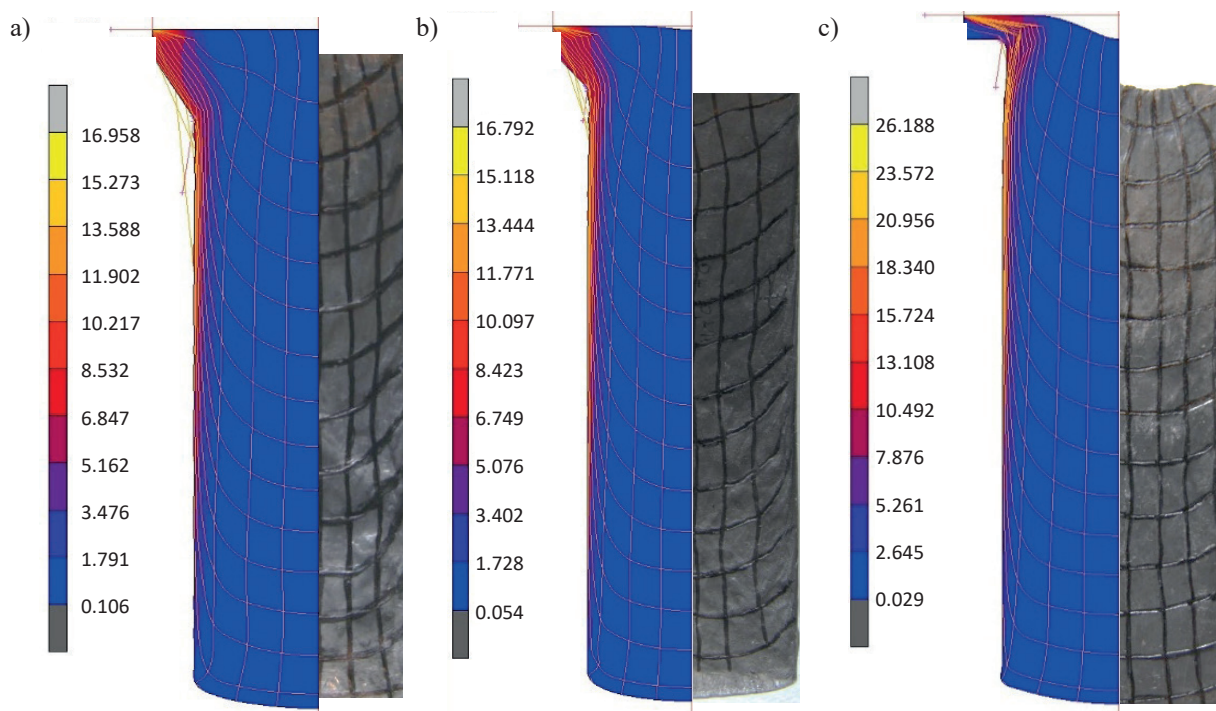


Fig. 9. Comparison of deformed meshes for samples deformed at 30° (a), 45° (b), 90° (c) angle convergence of die

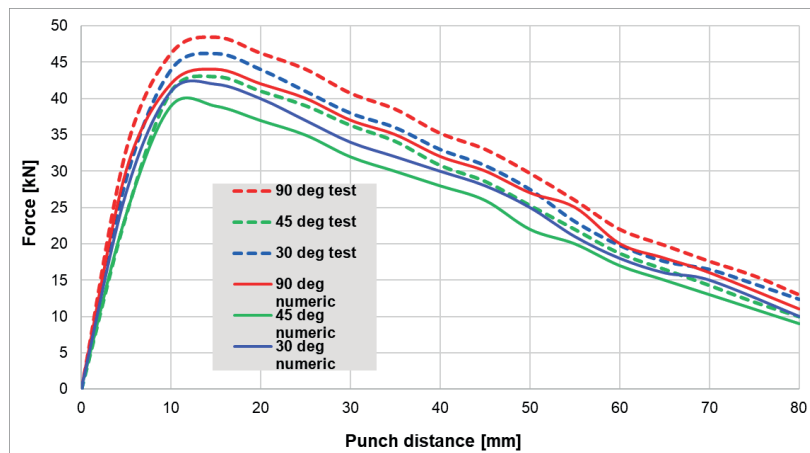


Fig. 10. Comparison of extrusion forces as a function of punch path for different die convergence angles between FEM and experimental results

Analyzing the above comparisons of FEM results and laboratory experiments, one can observe very large similarities in the way in which the material flows. Some differences may result from, for example, the inaccurate production of lead samples or careless application of coordination grids, which, in relation to numerical models (nearly ideal geometrically), may be the cause of discrepancies. Another issue is the tribological conditions, which also significantly determine the deformation of the material. It is essential to note that during the laboratory extrusion process, the tribological conditions change dynamically and may differ significantly from those assumed in numerical modelling. Figure 10 presents comparisons of extrusion forces obtained from FEM and from experimental tests.

In the case of the analysis of the force curves between FEM and experiments, a high level of agreement can be observed, although some shifts can be seen at the beginning of the process and in the final phase. The differences in the initial force range most likely result from the mismatch of the samples used in the experiments (differences in dimensions in relation to the recipient). In turn, the differences in the final range result from the fact that the experiments were carried out at ambient temperature, and the ambient temperature is the temperature of plastic heat treatment. This can cause the lead to weaken, which is manifested by a decrease in force at the end of the process. In turn, when it comes to the extrusion force curves for different angles, the lowest force values can be observed for an angle of 45°, both for the FEM results and the results from the experiments. The highest values occur for right angles in both cases. However, when it comes to the greatest plastic deformations, the highest values appear for right angles. The extrusion force in the case of the process carried out in real conditions for a convergence angle

of 90° is at a slightly higher level. For such deformation conditions, the obtained course of the extrusion force is about 10% higher than for the numerical model. Presumably, the reason for these differences was the assumption of a constant value of the friction coefficient for all tools in the mathematical modelling process. In the real process, probably as a result of high pressures and rupture of the lubricant film in the area of the die cavity, a discontinuity of the lubricant layer appears, and the friction coefficient reaches values higher than 0.05, as assumed in the modeling. Additionally, the material moved on the die surface in the mathematical modelling, while a small dead zone was observed to form in the die corners in the real process. It should be clearly emphasized that no dead zone was observed in the die corners in the numerical modelling. Only for the 90° angle, based on the “flow lines”, can the accumulation and overlap of the flow lines be observed. However, this is not an obvious dead zone, which should have appeared already at angles greater than 45°.

4.3. Forward extrusion process of aluminum

To highlight and identify the dead zone, the next stage involved building a numerical model for the co-rotating extrusion of Al and conducting verification tests under semi-industrial conditions. Numerical modeling was carried out for the Al alloy for a die convergence angle of 60°, which is different than for lead extrusion. This convergence value was adopted due to the fact that during Pb extrusion, for angles greater than 45°, a dead zone should appear, which was not observed in numerical modeling. Numerical simulations were conducted to create a dead zone during numerical modelling and to better characterize it. The stress-strain curves of aluminum

have been presented in tabular form, providing data for various strain values, strain rates, and temperatures. As in the case of numerical modeling of concurrent extrusion of aluminum, a constant friction coefficient of 0.05 for different tools was assumed (Fig. 11). In the actual physical process, due to improper lubrication, discontinuities in the lubricant layer may occur in the die area, leading to significantly higher friction coefficients.

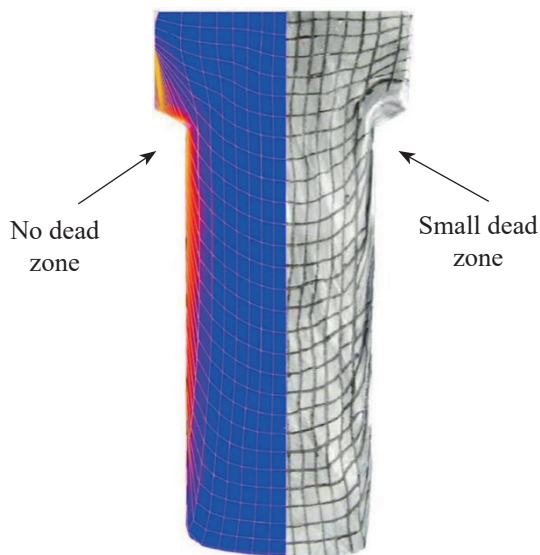


Fig. 11. The material flow pattern obtained from the finite element method (FEM) is represented as a special mesh, known as ‘flow lines’, as well as in the actual process

Moreover, the friction conditions are identical for all tools. The insertion forces as a function of displacement differed by about 20% under these friction conditions (Fig. 11a). Therefore, further numerical simulations were conducted at higher friction coefficient values. Ultimately, a similar material flow pattern and extrusion force profile were obtained in both the mathematical model and the real process when different friction coefficients were applied to each tool. A coefficient

of 0.05 was used for the punch, 0.1 for the container, and 0.25 for the die. Figure 12b shows the force profiles as a function of punch travel for the new friction conditions in mathematical modelling and for the real process, demonstrating significant agreement.

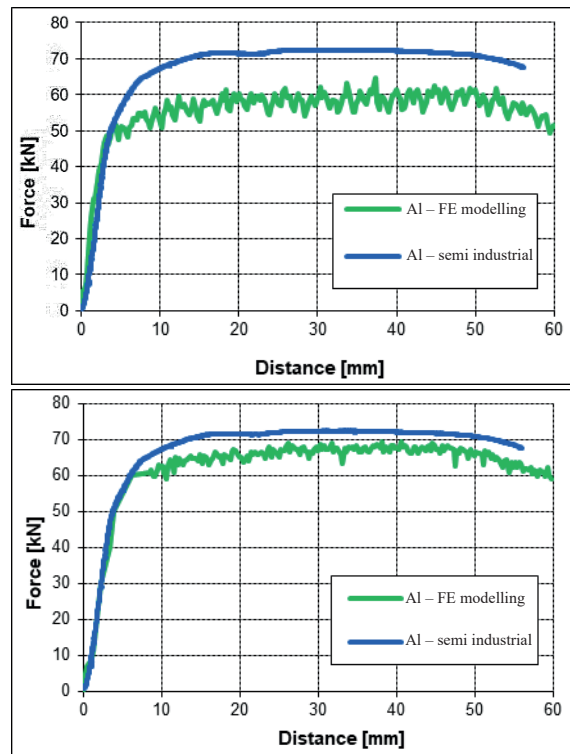


Fig. 12. Comparison of forces: a) the course of extrusion force as a function of punch travel for the real process and that obtained from the numerical model; b) extrusion forces as a function of punch travel for the real process and that obtained from the numerical model after correcting the friction coefficient

For a more comprehensive analysis, both the similarity in material flow and the strain distribution were evaluated using the ASAME image analysis program and results obtained from FEM (Fig. 13).

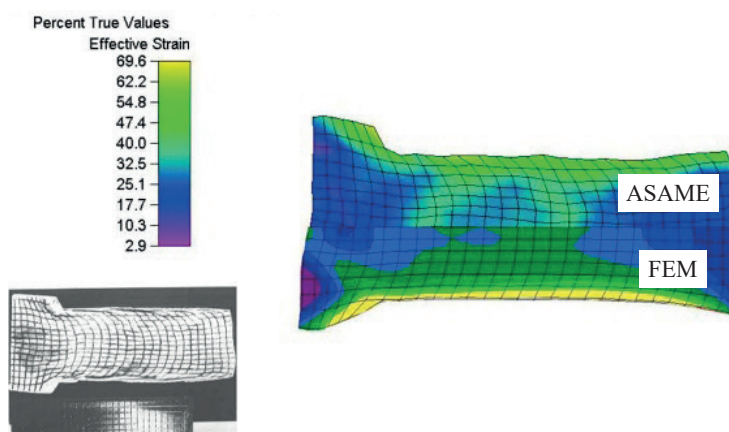


Fig. 13. Equivalent strain distributions obtained from the finite element method (FEM) and determined using the ASAME program for the actual process

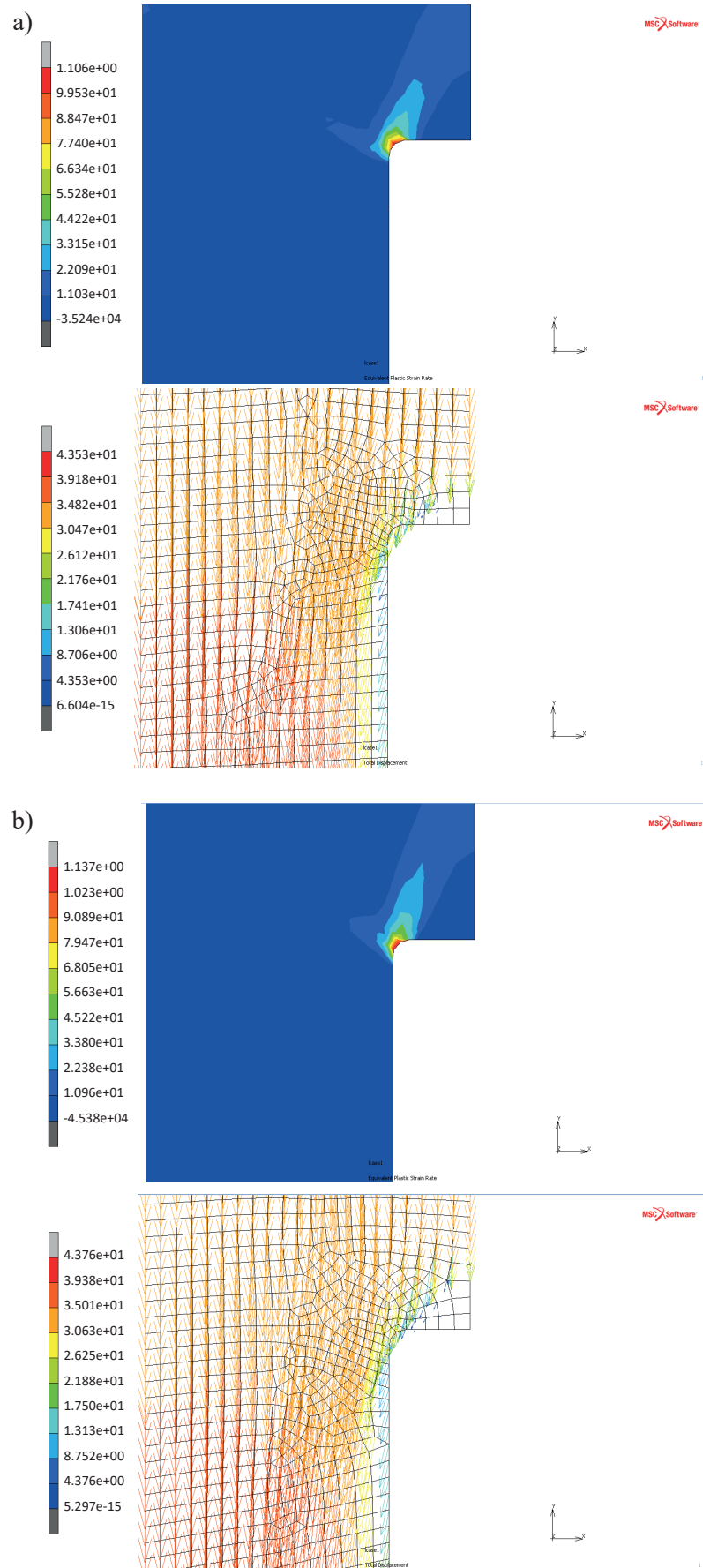


Fig. 14. The FEM results of the strain rate distributions (upper) and displacement vectors (bellow) for:
a) variant I – a constant low friction coefficient of 0.05; b) variant II – different friction for tools

As can be observed, tuning the numerical model by adjusting the tribological conditions (introducing different friction coefficients for various tools) resulted in very similar deformation of the coordinate grids and distributions of plastic deformation in both cases. The conducted research has shown that it is essential to check and verify boundary (tribological) conditions during the design and analysis of plastic forming processes, in this case, extrusion.

In order to conduct a deeper analysis of this phenomenon, numerical modelling was performed for the forward extrusion process with a die convergence angle of 90° , a small and uniform friction coefficient of 0.05 for all tools, as well as for higher friction coefficient values (0.1 for the punch, 0.1 for the container, and 0.25 for the die). In Figure 14, the strain rate distributions and displacement vectors are shown for two selected variants.

An analysis of the obtained results, particularly the displacement distributions, reveals that a small dead zone forms in the corner at low friction values. This zone becomes significantly more pronounced at higher friction coefficients (Fig. 14b), as highlighted by the red ellipses. This confirms that for low friction conditions, the dead zone is virtually negligible or not observed at all (Fig. 14a). In the real process, due to improper lubrication, discontinuities in the lubricant layer may occur in the die area, leading to significantly higher friction coefficients.

5. Summary and conclusion

This study addresses a crucial issue related to the impact of die convergence angles in the concurrent extrusion process. Numerical modelling of the process has provided significant insights into various aspects, including forging forces, plastic deformations, equivalent stresses, and material flow. Subsequent laboratory experiments confirmed the assumptions made in the Finite Element Method (FEM) modelling. The numerical modelling yielded valuable information that facilitated the selection and development of appropriate tool designs for other processes conducted under laboratory conditions. Additionally, the comprehensive research and development work conducted underscores the need to verify initial boundary condi-

tions in numerical modelling when analyzing, designing, or optimizing industrial material forming processes.

Based on the research conducted, the following key conclusions can be drawn:

- The analysis of strain distribution (minimal strains) and flow lines based on FEM and experiments indicate that the most optimal material deformation conditions occur at a 45-degree angle.
- In terms of extrusion forces, it is observed that the average force values for different convergence angles are lowest at a 45-degree angle, while the highest average forces are observed at a right angle. This is consistent in both numerical modelling and semi-industrial tests, where a dead zone likely forms in the corner.
- Utilizing digital image analysis programs allows for rapid comparison of results obtained from numerical modelling with the actual process.
- When comparing coordination grids from modelling with flow lines of deformed metals (lead and aluminum) obtained from the ASUME program, a high degree of consistency in results was achieved, confirming the validity of the research conducted and the assumptions made in FEM.

The conducted research showed great potential for using numerical techniques to analyze and improve extrusion processes. However, as the research showed, adopting certain simplifications in the model or having low experience as an engineer or technologist may result in obtaining incorrect results. The obtained results show the need to validate numerical models through semi-industrial experiments or other methods, such as physical modelling, to ensure their accuracy and reliability. Assuming constant tribological conditions may not reflect the actual process conditions, including the formation of dead zones for angles greater than 45° . Through detailed analysis of the actual process and material flow, variables and different friction coefficients, other than originally assumed, were introduced for each tool. Only then was the dead zone achieved in the modelling. The results of research works using FEM can also be applied to more advanced analyses, such as the detection of potential defects in the forming process, and may also be used in the future for analyzing the durability of tools and equipment in forging and extrusion processes.

References

- Brough, D., & Jouhara, H. (2020). The aluminium industry: A review on state-of-the-art technologies, environmental impacts and possibilities for waste heat recovery. *International Journal of Thermofluids*, 1–2, 100007. <https://doi.org/10.1016/j.ijft.2019.100007>
- Çalım, F., Güllü, A., Soydan, C., & Yüksel, E. (2023). State-of-the-art review for lead extrusion dampers: development, improvement, characteristics, application areas, and research needs. *Structures*, 58, 105477. <https://doi.org/10.1016/j.istruc.2023.105477>

- Campana, R. C., Vieira, P. C., & Plaut, R. L. (2010). Applicability of Adaptive Neural Networks (ANN) in the extrusion of aluminum alloys and in the prediction of hardness and internal defects. *Materials Science Forum*, 638–642, 303–309. <https://doi.org/10.4028/www.scientific.net/MSF.638-642.303>
- Chan, W. L., Fu, M. W., & Lu, J. (2008). An integrated FEM and ANN methodology for metal-formed product design. *Engineering Applications of Artificial Intelligence*, 21(8), 1170–1181. <https://doi.org/10.1016/j.engappai.2008.04.001>
- Chenot, J.-L., & Fourment, L., Ducloux, R., & Wey, E. (2010). Finite element modelling of forging and other metal forming processes. *International Journal of Material Forming*, 3(1), 359–362. <https://doi.org/10.1007/s12289-010-0781-5>
- Donati, L., Reggiani, B., Pelaccia, R., Negozio, M., & Di Donato, S. (2022). Advancements in extrusion and drawing: A review of the contributes by the ESAFORM community. *International Journal of Material Forming*, 15, 41. <https://doi.org/10.1007/s12289-022-01664-w>
- Hawryluk, M., & Rychlik, M. (2022). An implementation of robotization for the chosen hot die forging process. *Archives of Civil and Mechanical Engineering*, 22, 119. <https://doi.org/10.1007/s43452-022-00448-y>
- Hawryluk, M., Lachowicz, M., Zwierzchowski, M., Janik, M., Gronostajski, Z., & Filipiak, J. (2023). Influence of the grade of hot work tool steels and its microstructural features on the durability of punches used in the closed die precision forging of valve forgings made of nickel-chrome steel. *Wear*, 528–529, 204963. <https://doi.org/10.1016/j.wear.2023.204963>
- He, Z., Wang, H.-n., Wang, M.-j., & Li, G.-y. (2012). Simulation of extrusion process of complicated aluminium profile and die trial. *Transactions of Nonferrous Metals Society of China*, 22(7), 1732–1737. [https://doi.org/10.1016/S1003-6326\(11\)61380-0](https://doi.org/10.1016/S1003-6326(11)61380-0)
- Hu, Ch.-l., Meng, L.-f., Zhao, Z., Gu, B., & Cai, B. (2012). Optimization for extrusion process of aluminum controller housing. *Transactions of Nonferrous Metals Society of China*, 22(supl. 1), 48–53. [https://doi.org/10.1016/S1003-6326\(12\)61682-3](https://doi.org/10.1016/S1003-6326(12)61682-3)
- Ji, H., Qiao, J., Kang, N., Wang, X., & Huang, J. (2023). Optimization of hot extrusion process parameters for 7075 aluminum alloy rims based on HyperXtrude. *Journal of Materials Research and Technology*, 25, 4918–4928. <https://doi.org/10.1016/j.jmrt.2023.06.239>
- Khalid, M. Y., Umer, R., & Khan, K. A. (2023). Review of recent trends and developments in aluminium 7075 alloy and its metal matrix composites (MMCs) for aircraft applications. *Results in Engineering*, 20, 101372. <https://doi.org/10.1016/j.rineng.2023.101372>
- Kochański, A., Kozłowski, J., Perzyk, M., & Sałowska, H. (2024). Data-driven advisory system for industrial manufacturing. Application to the aluminum extrusion process. *Knowledge-Based Systems*, 294, 111631. <https://doi.org/10.1016/j.knsys.2024.111631>
- Leśniak, D., Zasadziński, J., Libura, W., Gronostajski, Z., Śliwa, R., Leszczyńska-Madej, B., Kaszuba, M., Woźnicki, A., Płonka, B., Widomski, P., & Madura, J. (2024). Latest advances in extrusion processes of light metals. *Archives of Civil and Mechanical Engineering*, 24, 184. <https://doi.org/10.1007/s43452-024-00988-5>
- Liu, G., & Müller, D. B. (2012). Addressing sustainability in the aluminum industry: A critical review of life cycle assessments. *Journal of Cleaner Production*, 35, 108–117. <https://doi.org/10.1016/j.jclepro.2012.05.030>
- Madej, L., Tokunaga, T., Matsuura, K., Ohno, M., & Pietrzyk, M. (2015). Physical and numerical modelling of backward extrusion of Mg alloy with Al coating. *CIRP Annals*, 64(1), 253–256. <https://doi.org/10.1016/j.cirp.2015.04.085>
- Negozio, M., Ferraro, V., Donati, L., & Lutey, A. H. A. (2024). Predicting grain size in extruded AA6063 profiles: A unified approach based on finite element analysis and machine learning. *The International Journal of Advanced Manufacturing Technology*, 133, 4543–4560. <https://doi.org/10.1007/s00170-024-14021-9>
- Oberhausen, G., Zhu, Y., & Cooper, D. R. (2022). Reducing the environmental impacts of aluminum extrusion. *Resources, Conservation and Recycling*, 179, 106120. <https://doi.org/10.1016/j.resconrec.2021.106120>
- Parvizian, F., Kayser, T., Hortig, Ch., & Svendsen, B. (2008). Thermomechanical modeling and simulation of aluminum alloys during extrusion process. *Proceedings in Applied Mathematics and Mechanics*, 8(1), 10517–10518. <https://doi.org/10.1002/pamm.200810517>
- Soydan, C., Çalım, F., Güllü, A., & Yüksel, E. (2024). Experimental investigation of the effective parameters on the lead extrusion damper performance. *Engineering Structures*, 318, 118714. <https://doi.org/10.1016/j.engstruct.2024.118714>
- The Engineering ToolBox (2003). *Understanding Convective Heat Transfer: Coefficients, Formulas & Examples*. https://www.engineeringtoolbox.com/convective-heat-transfer-d_430.html
- Vazquez, V., & Altan, T. (2000). New concepts in die design – physical and computer modeling applications. *Journal of Materials Processing Technology*, 98(2), 212–223. [https://doi.org/10.1016/S0924-0136\(99\)00202-2](https://doi.org/10.1016/S0924-0136(99)00202-2)
- Williams, A. J., Croft, T. N., & Cross, M. (2002). Computational modelling of metal extrusion and forging processes. *Journal of Materials Processing Technology*, 125–126, 573–582. [https://doi.org/10.1016/S0924-0136\(02\)00401-6](https://doi.org/10.1016/S0924-0136(02)00401-6)
- Yang, D. Y., Ahn, D. G., Lee, C. H., Park, C. H., & Kim, T. J. (2002). Integration of CAD/CAM/CAE/CP for the development of metal forming process. *Journal of Materials Processing Technology*, 125–126, 26–34. [https://doi.org/10.1016/S0924-0136\(02\)00414-4](https://doi.org/10.1016/S0924-0136(02)00414-4)
- Zhang, C., Zhao, G., Chen, H., Guan, Y., & Li, H. (2012). Optimization of an aluminum profile extrusion process based on Taguchi's method with S/N analysis. *The International Journal of Advanced Manufacturing Technology*, 60, 589–599. <https://doi.org/10.1007/s00170-011-3622-x>

